DOI: 10.1002/ejoc.200900775

Aplysqualenols A and B: Squalene-Derived Polyethers with Antitumoral and Antiviral Activity from the Caribbean Sea Slug *Aplysia dactylomela*

Brunilda Vera,[a] Abimael D. Rodríguez,*[a] Edward Avilés,[a] and Yasuyuki Ishikawa[a]

Dedicated respectfully to Professor Alex Nickon[‡]

Keywords: *Aplysia dactylomela* / Aplysqualenols A and B / Natural products / Structure elucidation / Polyethers / Biological activity

The novel bromotriterpene polyethers aplysqualenol A (**1**) and B (**2**) have been isolated from the Caribbean sea slug *Aplysia dactylomela*, collected in Puerto Rico, and their structures and relative configurational assignments established from spectroscopic data aided by quantum mechanical calculations of NMR chemical shifts. Although both these compounds may be conceived as polyoxacyclic derivatives of the C_{30} squalene skeleton, it is notable that **1** and **2** each possess an unprecedented C15-to-C24 flexible chain of (14*S**) spatial disposition that contains a unique ether bridge between C16 and C19. Biological activity screening tests revealed that, although aplysqualenol A (**1**) does not have significant antiinfective properties, it possesses potent antitumoral and antiviral activities.

Introduction

Previous chemical investigations of the Caribbean sea slug *Aplysia dactylomela* Rang (order Anaspidea, family Aplysiidae), found worldwide in tropical to warm temperate waters, reported the isolation of two principal groups of compounds: terpenes (monoterpenes, sesquiterpenes, diterpenes, and steroids) and nonterpenoid C_{15} acetogenins.[1] To date, over 60 terpenoidal natural products have been isolated from *A. dactylomela*, and they have exhibited various biological activities including anticancer, anti-HIV, alguicidal, ichthyotoxic, nematicidal, antiplasmodial, and antibacterial activities.[2] As part of a recent exploratory survey of marine invertebrates for anticancer constituents, *A. dactylomela* was collected in Cabo Rojo, Puerto Rico (April 2001), and extracts from this anaspidean mollusk gave evidence of significant cytotoxic activity in the brine shrimp lethality bioassay (BSLT).[3] Further examination of its constituents resulted in the isolation of two cytotoxic and structurally unique organic compounds. Here we report the isolation and structure determination of aplysqualenols A (**1**) and B (**2**), novel brominated triterpene polyethers with tetracyclic skeletons, isolated from two specimens of this chemically prolific animal.[4]

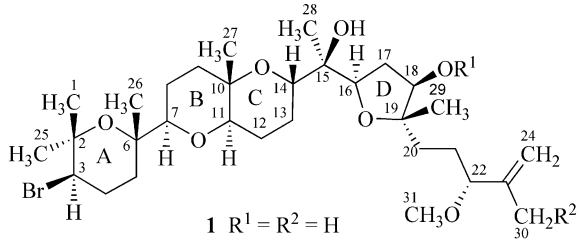

1 $R^1 = R^2 = H$
2 $R^1 = H$, $R^2 = OH$
3 $R^1 = Ac$, $R^2 = H$
4 $R^1 = Ac$, $R^2 = OAc$

The MeOH/$CHCl_3$ (1:1) extract of freeze-dried *A. dactylomela* (54 g, dry weight) was partitioned between hexane and H_2O. The hexane-soluble material, which exhibited potent cytotoxicity against *Artemia salina*,[3] was subjected to fractionation by column chromatography (silica gel) and polar bonded-phase HPLC to afford aplysqualenol A (**1**) and aplysqualenol B (**2**) as colorless oils (0.06% and 0.02% yields, respectively, based on crude extract weight). Aplysqualenol A (**1**) was evaluated in the National Cancer Institute (NCI) three-cell-line, one-dose primary anticancer assay and displayed potent in vitro cytotoxicity against MCF-7 breast cancer, NCI-H460 nonsmall-cell lung cancer, and SF-268 CNS cancer (the percentages of growth of the treated cells in relation to untreated cells were approximately 0, 0, and 4%, respectively).

[a] Department of Chemistry, University of Puerto Rico,
P. O. Box 23346, U. P. R. Station, San Juan, PR 00931-3346
Fax: +1-787-756-8242
E-mail: abrodriguez@uprrp.edu
[‡] Vernon K. Krieble Professor Emeritus of Chemistry at Johns Hopkins University
Supporting information for this article is available on the WWW under http://dx.doi.org/10.1002/ejoc.200900775.

Results and Discussion

The molecular formula of aplysqualenol A {**1**, $[\alpha]_D^{20}$ = +48.1 (c = 1.6, $CHCl_3$)} was determined to be $C_{31}H_{53}BrO_7$ by HR-FAB-MS and ^{13}C NMR spectroscopy. Treatment of **1** with acetic anhydride and pyridine at 55 °C for 5 h gave the corresponding monoacetate **3** [$C_{33}H_{55}BrO_8$, $\tilde{\nu}_{max}$ = 1740 cm^{-1} and δ_H = 2.05 ppm (s, 3 H)], the IR spectrum of which still showed an absorption due to a hydroxy group at 3549 cm^{-1}, thus demonstrating the presence of secondary and tertiary hydroxy groups in **1**. The presence of two hydroxy groups was further indicated by two D_2O-exchangeable resonances (δ = 2.97 and 3.47 ppm) in the ^1H NMR spectrum. The ^1H and ^{13}C NMR spectroscopic data revealed that aplysqualenol A (**1**) possesses seven tertiary methyl groups, five oxygenated quaternary carbon atoms, six oxygenated methine carbon atoms, and a brominated methine carbon atom (δ = 58.9 ppm). Because aplysqualenol A displayed signals for only one unsaturated bond [δ_C = 144.4 (C) and 113.8 ppm (CH_2); δ_H = 4.87 (br. s, 1 H) and 4.93 ppm (br. s, 1 H)], **1** was assumed to contain four oxacyclic units. Detailed analysis of the ^1H-^1H COSY, HMQC, and HMBC spectra of **1** showed the presence of the same partial structural units in the molecule (rings A–B–C) as had been found in thyrsiferol (**5**) and venustatriol (**6**), isolated from red algae of the genus *Laurencia*,[5,6] and also in aplysiols A (**7**) and B (**8**), recently isolated from South China Sea specimens of *A. dactylomela*.[7] Furthermore, the ^1H-^1H COSY and HMBC data, summarized in Table 1, allowed the foregoing partial structures (C1

Table 1. ^1H NMR (500 MHz), ^{13}C NMR (125 MHz), ^1H-^1H COSY, HMBC, and NOESY spectroscopic data for aplysqualenol A (**1**) in $CDCl_3$.[a]

Atom	δ_H, mult, integr (J in Hz)	δ_C (mult)[b]	^1H-^1H COSY	HMBC[c]	NOESY
1	1.40, s	23.6 (CH_3)		H3, H25	H4α, H25, H26
2		75.0 (C)		H1, H3, H4αβ, H25	
3	3.88, dd, 1 H (4.0, 12.3)	58.9 (CH)	H4αβ	H1, H4αβ, H5αβ, H25	H4α, H25
4α	2.10, dq, 1 H (3.9, 4.0, 4.5, 13.5)	28.3 (CH_2)	H3, H4β, H5αβ		H3, H4β
4β	2.22, dq, 1 H (3.5, 12.3, 13.1, 13.5)		H3, H4α, H5αβ		H1, H4α, H26
5α	1.82, m, 1 H	37.1 (CH_2)	H4αβ, H5β	H26	H5β, H7
5β	1.53, m, 1 H		H4αβ, H5α		H5α, H26
6		74.3 (C)		H4αβ, H7, H8α, H26	
7	3.09, dd, 1 H (2.2, 10.9)	86.9 (CH)	H8αβ	H9β, H26	H5α, H8α, H9α, H11
8α	1.53, m, 1 H	22.9 (CH_2)	H7, H8β, H9αβ	H9α	H7, H8β
8β	1.78, m, 1 H		H7, H8α, H9αβ		H8α, H26, H27
9α	1.53, m, 1 H	37.5 (CH_2)	H8αβ, H9β	H27	H7, H9β, H11
9β	1.73, m, 1 H		H8αβ, H9α		H9α, H27
10		73.0 (C)		H8αβ, H9αβ, H27	
11	3.01, dd, 1 H (3.8, 11.4)	80.8 (CH)	12αβ	H9β, H27	H7, H9α, H13α
12α	1.66, m, 1 H	24.3 (CH_2)	H11, H13αβ	H14	
12β	1.53, m, 1 H		H11, H13αβ		H14, H27
13α	1.50, m, 1 H	26.0 (CH_2)	H12αβ, H14		H11, H28
13β	1.65, m, 1 H		H12αβ, H14		
14	3.54, dd, 1 H (2.5, 11.6)	72.5 (CH)	H13αβ	H13αβ, H28	H12β, H27, H29
15		74.9 (C)		H13αβ, H14, 15-OH, H16, H17αβ, H28	
16	3.85, dd, 1 H (4.2, 9.1)	79.1 (CH)	H17αβ	H17α, H18, H28	H17α, H18, H28
17α	2.34, ddd, 1 H (6.0, 8.9, 14.3)	35.3 (CH_2)	H16, H17β, H18		H16, H17β, H18
17β	1.96, dd, 1 H (3.0, 14.3)		H16, H17α, H18		H17α, 18-OH, H28
18	3.81, dd, 1 H (2.0, 5.9)	75.8 (CH)	H17αβ, 18-OH	H17β, 18-OH, H20β, H29	H16, H17α, H20α, H30
19		85.7 (C)		H17β, H20αβ, H29	
20α	1.40, m, 1 H	34.1 (CH_2)	H20β, H21αβ	H21αβ, H22, H29	H18, H20β
20β	1.30, dd, 1 H (4.8, 12.3)		H20α, H21αβ		H20α
21αβ	1.64, m, 1 H, 1.56, m, 1 H	28.2 (CH_2)	H20αβ, H22		H29
22	3.44, dd, 1 H (6.5, 6.8)	86.1 (CH)	H21αβ	H20αβ, H21αβ, H24αβ, H30, OCH_3	H24α, H30, OCH_3
23		144.4 (C)		H30	
24α	4.87, br. s, 1 H	113.8 (CH_2)	H24β, H30	H22, H30	H22, H24β
24β	4.93, br. s, 1 H		H24α, H30		H24α, H30
25	1.27, s, 3H	31.0 (CH_3)		H1, H3	H1, H3
26	1.20, s, 3H	20.1 (CH_3)			H1, H4β, H5β, H8β
27	1.15, s, 3H	14.8 (CH_3)		H11	H8β, H9β, H12β, H14
28	1.17, s, 3H	18.1 (CH_3)			H13α,15-OH, H16, H17β
29	1.22, s, 3H	19.4 (CH_3)			H14, 18-OH, H21β
30	1.63, s, 3H	16.3 (CH_3)	H24αβ	H22, H24αβ	H18, H22, H24β, OCH_3
OCH_3	3.19, s, 3H	56.0 (CH_3)		H22	H22, H30
15-OH	2.97, br. s, 1 H				H28
18-OH	3.47, br. d, 1 H (7.3)		H18		H17β, H29

[a] Spectra were recorded at 25 °C. Chemical shift values are in parts per million (ppm) relative to the residual $CHCl_3$ (δ = 7.25 ppm) or $CDCl_3$ (δ = 77.0 ppm) signals. [b] ^{13}C NMR multiplicities were obtained from APT experiments. [c] Protons correlated to carbon resonances in the ^{13}C column. Parameters were optimized for $^{2,3}J_{C,H}$ = 6 and 8 Hz.

through C15 and C25 through C28) and the remaining ring system D (C16 through C24 and C29 through C31) to be connected, establishing the connectivities of all the carbon atoms in **1** as shown.

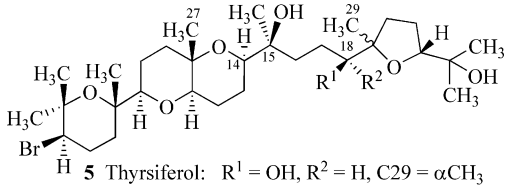

5 Thyrsiferol: R^1 = OH, R^2 = H, C29 = αCH_3

6 Venustatriol: R^1 = H, R^2 = OH, C29 = βCH_3

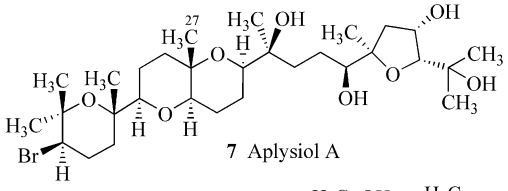

7 Aplysiol A

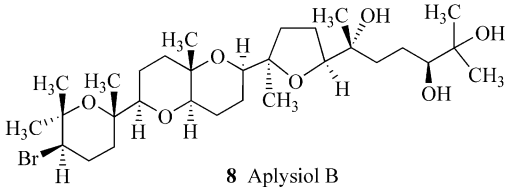

8 Aplysiol B

This unprecedented architecture required further confirmation, which was provided by unambiguous determination of the locations of the two hydroxy groups in **1**. The positions of these pivotal functionalities were initially determined by HMBC correlations (C15/15-OH and C18/18-OH) and were later confirmed by a deuterium shift experiment, which revealed that, out of all the oxygenated carbon atoms, only the two signals for C15 and C18 were shifted significantly to lower field when measured in CD_3OH rather than CD_3OD.[8] Having definitively located the two hydroxy groups at C15 and C18, we inferred that the other nine oxacarbon moieties in aplysqualenol A all participate in ether linkages. The locus of oxolane ring D, arising from an ether bridge between C16 and C19, was thus indicated by the HMBC correlations (C15/H-16, C15/H-17αβ, C16/H-18, C16/H_3-28, C19/H-17β, C19/H-20αβ, and C-19/H_3-29). The one additional ethereal group (-OCH_3) present in **1** was shown to be located at C22 on the basis of the HMBC correlations (C22/-OCH_3, C22/H-24αβ, C22/H_3-30, and C22/H-21αβ), leaving the bromine atom to reside at C3.

The oxacyclic systems of **1** were also deduced from the specific fragment ions in the EI mass spectrum (Figure 1). The mass spectrum showed fragment ions at *m*/*z* = 503/505 $[M - C_7H_{13}O]^+$, 403/405 $[M - C_{12}H_{21}O_3]^+$, 359/361 $[M - C_{14}H_{25}O_4]^+$, and 205/207 $[M - C_{23}H_{39}O_6]^+$, due to cleavage at the C19–C20, C15–C16, C14–C15, and C6–C7 bonds, respectively. The remaining two ether linkages hence consisted of a 2,7-dioxabicyclo[4.4.0]decane ring, as was evident from the intense (100%) fragment ion at *m*/*z* = 153 $[C_9H_{13}O_2]^+$. The presence of an oxolane ether bridge encompassing positions C16 and C19 was corroborated by the rearranged fragment ion at *m*/*z* = 214 $[M - C_{19}H_{32}BrO_4 + H]^+$ resulting from cleavage of the C15–C16 bond. Furthermore, the fragment ion at *m*/*z* = 257 $[M - C_{17}H_{28}BrO_3]^+$, arising from cleavage at C14–C15, confirmed the presence in **1** of the partial structural unit from C15 through C24 (including C28 through C31). Consequently, aplysqualenol A (**1**) was found to be a new member of the class of squalene-derived bromotriterpenes with novel structural features not found in known congeners of this class of natural products.[4,7]

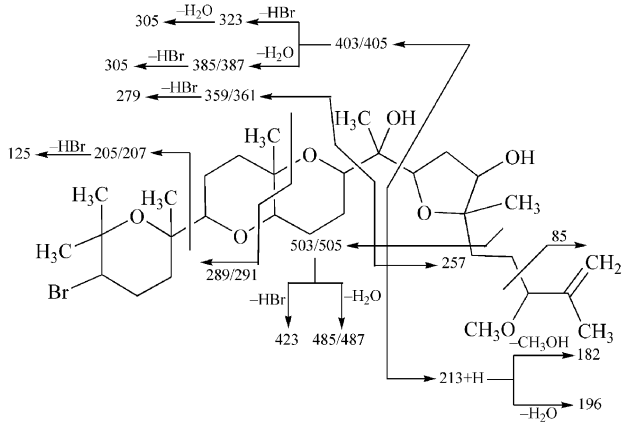

Figure 1. Diagnostic fragment ions (*m*/*z*) of aplysqualenol A (**1**) detected in the EI mass spectrum.

The assignment of the relative stereochemistry of **1**, except at C22, was straightforward. The equatorial orientation of the bromine atom at C3 on the A ring was evident from the *J* values, with a vicinal axial–axial coupling constant of H-3 (12.3 Hz) in the ^{1}H NMR spectrum of **1**. From this point forward, the relative stereochemistries were determined from the NOESY spectrum as summarized in Table 1. NOEs about the ABC rings were detected between H-3/H_3-25, H_3-1/H_3-26, H-5α/H-7, H_3-26/H-8β, H-7/H-11, H-14/H-12β, and, most importantly, H-14/H_3-27, establishing *cis* relationships between these sets of protons. No NOE, however, was detected between H-7/H_3-26, H-11/H_3-27, or H-11/H-14, thus suggesting that these pairs of protons are *trans*-oriented. In addition, NOEs about the C/D rings were detected between H-13α/H_3-28, H-16/H_3-28, H-16/H-17α, H-17α/H-18, and H-14/H_3-29, suggesting close spatial proximities for these protons. Moreover, the lack of NOEs between H14/H_3-28, H-14/H-16, H-16/H_3-29, and H-18/H_3-29 suggested that the stereochemical arrangements of these proton pairs were *trans* (Figure 2). The observation that in compound **1** the proton signal for H-14 was resolved as a doublet of doublets with two different coupling constant values (one much larger than the other, indicating a chair/chair B–C ring system) confirmed the axial orientation of this methine group and, therefore, that the relative stereochemistry at C-14 in aplysqualenol A (**1**) would be (*S**). As far as we know, this is the first example of a squalene polyether derivative displaying a C15-to-C24 flexible side chain with an equatorial spatial disposition.[9]

In order to corroborate the relative configuration shown for aplysqualenol A, molecular mechanics/dynamics calculations were performed to establish the dominant confor-

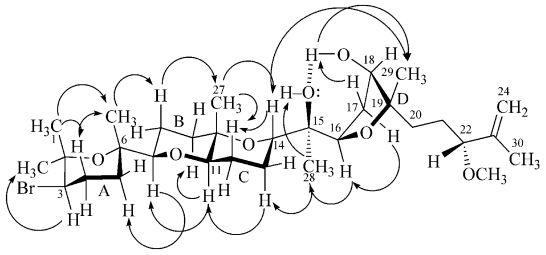

Figure 2. Plausible conformations of rings A–B–C–D in **1** showing selected NOESY correlations.

mations of **1**.[10] The results of the conformational analysis implied that the secondary alcohol at C18 was fixed with the tertiary hydroxy oxygen atom at C15 in a hydrogen bond. In turn, 15-OH is hydrogen-bonded to the oxygen atom of oxane ring C. Indeed, the presence of intramolecular hydrogen bonding in aplysqualenol A was supported experimentally by the strong couplings of H-18 and 18-OH observed in the ^{1}H-^{1}H COSY spectrum, by the fact that acetylation of **1** did not take place at 25 °C, and by the strong NOEs detected between H_3-28/15-OH, H-17β/18-OH, and H_3-29/18-OH. Furthermore, the coupling constants of H-22 with the diastereotopic protons H_2-21 ($J_{22,21\alpha}$ = 6.5 Hz and $J_{22,21\beta}$ = 6.8 Hz) indicated that free rotation about the C21–C22 bond renders them equivalent, thus strengthening the contention that the secondary alcohol is fixed in a hydrogen bond with 15-OH and not with the methoxy ether at C22. Insofar as the relative configuration for C22 is concerned, it was ultimately assigned as (*R**) on the basis of a combined approach that included NOESY NMR spectroscopic data acquired with aplysqualenol B (**2**), an integrated QM-NMR (Quantum Mechanical-NMR) approach based on DFT (density functional theory)[11] calculations of ^{13}C NMR chemical shifts, and the analysis of the experimentally measured NMR spectroscopic data for aplysqualenol A (**1**), as well as biogenetic considerations (vide infra). Figure 2 shows a plausible conformation of rings A–D based on the observed coupling constants and NOE correlations, which indicated the relative stereochemistry of aplysqualenol A (**1**) to be (3*R**, 6*S**,7*R**,10*S**,11*R**,14*S**,15*R**,16*R**,18*R**,19*S**,22*R**).[12] Sadly, all of our attempts to determine the absolute stereochemistry by mixing **1** with a solid matrix-bound auxiliary reagent (MTPA) directly in the NMR tube were unsuccessful.[13,14]

Compound **2** (aplysqualenol B) was also isolated as a colorless oil {$[\alpha]_D^{20}$ = +27.1 (*c* = 1.4, $CHCl_3$)}. Mass spectral analysis of this metabolite showed a molecular ion peak consistent with the molecular formula $C_{31}H_{53}BrO_8$ (found $[M + H]^+$ 633.3003; calcd. 633.3002). Assignment of the structure for this metabolite was aided by the considerable spectroscopic analogy to aplysqualenol A (**1**). The only significant variations in the ^{1}H NMR spectra of compounds **2** and **1** were the disappearance of the tertiary methyl signal ascribable in **1** to H_3-30 (δ_H = 1.63 ppm) and the appearance of a pair of AB doublets in **2** at δ_H = 4.21 (*J* = 13.5 Hz, 1 H) and 4.09 ppm (*J* = 14.3 Hz, 1 H), as well as the downfield shifts in the protons H-22 [δ_H = 3.62 ppm (dd, *J* = 6.5, 6.8 Hz)] and H_2-24 [δ_H = 5.06 (br. s, 1 H, H-24α) and 5.24 ppm (br. s, 1 H, H-24β)]. These data suggested that the modifications in this compound were mainly located in the C_6 side chain appended to ring D. The connectivities observed in ^{1}H-^{1}H COSY, HMQC, and HMBC experiments (Table 2) made it possible to assign the fragment C20-to-C24 (including C30) as follows: δ_C = 34.2 (CH_2, C20), 28.6 (CH_2, C21), 85.0 (CH, C22), 146.9 (C, C23), 114.0 (CH_2, C24) and 62.9 ppm (CH_2, C30). These observations can only be explained by the presence in **2** of a primary hydroxy group at C30. The isolated hydroxymethylene group is connected to the ring D side chain through C23 by HMBC correlations (C30/H-22, C30/H-24αβ, C23/H-30αβ and C24/H-30αβ). In confirmation of the presence of this system, compound **2** gave the 18,30-diacetate **4** [$C_{35}H_{57}BrO_{10}$, $\tilde{\nu}_{max}$ = 3541, 1740 cm^{-1} and δ_H = 2.05 (s, 3 H) and 2.10 ppm (s, 3 H)] after overnight treatment with Ac_2O/Py at 25 °C, thus confirming its structure as an aplysqualenol A derivative. As in compound **1**, strong NOE correlations established a *cis* orientation between the methyl group H_3-27 (δ_H = 1.15 ppm) and the oxymethine proton H-14 (δ_H = 3.54 ppm), indicating that the relative configuration at C14 in compound **2** is (*S**). The relative stereochemical arrangement of the remaining carbon atoms C3, C6, C7, C10, C11, C15, C16, C18, and C19 in compound **2** was established to be identical with that observed in aplysqualenol A (**1**) on the basis of the observed NOE data in the NOESY experiments in $CDCl_3$ (Table 2).

The relative stereochemistry of C22 in compound **2** was established as follows. The fact that in aplysqualenol B (**2**) the H_2-30 protons are diastereotopic (appearing as an isolated AB system indicating rotational constraints along the C23–C30 bond) implied that the primary alcohol was fixed with the methoxy ether oxygen atom in a hydrogen bond. This contention was supported by molecular mechanics calculations, which predicted identical coupling constant values between H-22 and the diastereotopic H_2-21 protons (actual values observed: $J_{22,21\alpha}$ = 6.5 Hz and $J_{22,21\beta}$ = 6.8 Hz) in the most stable conformation of compound **2** (Table 2). The NOE connectivities observed between H-22 and H-30β, H-24α, and, most importantly, H-16, and the observation that in diacetate derivative **4**, in which such hydrogen bonds are no longer attainable, the H_2-30 protons appeared as broad singlets centered near δ = 4.56 ppm, strongly supported the existence of such hydrogen bond.[15] The relative stereochemistry at C22 in this compound was thus established as (*R**). Because these compounds share the same biogenetic pathway, it is highly reasonable that the most likely configuration for aplysqualenol B (**2**) is (3*R**,6*S**,7*R**,10*S**,11*R**,14*S**,15*R**,16*R**,18*R**,19*S**,22*R**).

With the aim of strengthening the assignment of relative stereochemistry at the 11 stereogenic centers (C3, C6, C7, C10, C11, C14, C15, C16, C18, C19, and C22) in aplysqualenol A (**1**), we undertook a study of the configuration by an integrated QM-NMR approach based on DFT calculations of ^{13}C NMR chemical shifts and the analysis of the experimentally measured NMR spectroscopic data. Criti-

Table 2. ^{1}H NMR (500 MHz), ^{13}C NMR (125 MHz), ^{1}H-^{1}H COSY, HMBC, and NOESY spectroscopic data for aplysqualenol B (**2**) in $CDCl_3$.[a]

Atom	δ_H, mult, integr (*J* in Hz)	δ_C (mult)[b]	^{1}H-^{1}H COSY	HMBC[c]	NOESY
1	1.39, s	23.6 (CH_3)		H25	H4β, H25, H26
2		75.0 (C)		H1, H3, H25	
3	3.88, dd, 1 H (4.0, 12.3)	58.9 (CH)	H4αβ	H1, H4β, H5β, H25	H4α, H5α, H25
4α	2.09, dq, 1 H (3.8, 3.9, 4.1, 13.5)	28.2 (CH_2)	H3, H4β, H5αβ		H3, H4β, H5α
4β	2.24, dq, 1 H (3.7, 12.8, 13.1, 13.5)		H3, H4α, H5αβ		H1, H4α, H26
5α	1.81, m, 1 H	37.1 (CH_2)	H4αβ, H5β	H26	H4α, H5β, H7, H26
5β	1.52, m, 1 H		H4αβ, H5α		H5α, H26
6		74.3 (C)		H26	
7	3.10, dd, 1 H (2.2, 10.9)	86.9 (CH)	H8αβ	H8α, H9α, H26	H5α, H8α, H9α, H11
8α	1.52, m, 1 H	23.0 (CH_2)	H7, H8β, H9αβ		H7, H8β
8β	1.78, m, 1 H		H7, H8α, H9αβ		H8α, H26, H27
9α	1.50, m, 1 H	37.5 (CH_2)	H8αβ, H9β	H27	H7, H9β, H11
9β	1.72, m, 1 H		H8αβ, H9α		H9α, H27
10		73.0 (C)		H8α, H9β, H27	
11	3.01, dd, 1 H (3.9, 11.4)	80.7 (CH)	12αβ	H9β, H13β, H27	H7, H9α, H13α
12α	1.66, m, 1 H	24.3 (CH_2)	H11, H12β, H13αβ		H11
12β	1.53, m, 1 H		H11, H12α, H13αβ		H27
13α	1.48, m, 1 H	26.0 (CH_2)	H12αβ, H13β, H14		H11, H28
13β	1.61, m, 1 H		H12αβ, H13α, H14		
14	3.54, dd, 1 H (2.5, 11.7)	72.5 (CH)	H13αβ	H13α, H28	H27
15		75.0 (C)		H14, H17α, H28	
16	3.84, dd, 1 H (4.2, 9.1)	79.2 (CH)	H17αβ	H17α, H28	H17α, H22, H28
17α	2.33, ddd, 1 H (5.9, 9.1, 14.4)	35.2 (CH_2)[d]	H16, H17β, H18		H16, H17β, H18
17β	1.97, ddd, 1 H (1.3, 4.0, 14.4)		H16, H17α, H18		H17α, H28
18	3.80, br. m, 1 H	75.9 (CH)[d]	H17αβ, 18-OH	H17β, H29	H17α, H20α
19		85.7 (C)		H17β, H20α, H29	
20α	1.42, m, 1 H	34.2 (CH_2)	H20β, H21αβ	H22, H29	H18, H20β
20β	1.31, m, 1 H		H20α, H21αβ		H20α
21αβ	1.65, m, 2H	28.6 (CH_2)	H20αβ, H22	H22	
22	3.62, dd, 1 H (6.5, 6.8)	85.0 (CH)	H21αβ	H21αβ, H24αβ, OCH_3	H16, H24α, H30β, OCH_3
23		146.9 (C)		H24αβ, H30αβ	
24α	5.06, br. s, 1 H	114.0 (CH_2)	H24β	H22, H30αβ	H22, H24β, OCH_3
24β	5.24, br. s, 1 H		H24α		H24α, H30α
25	1.27, s, 3H	31.0 (CH_3)		H1	H1, H3
26	1.20, s, 3H	20.1 (CH_3)		H5α, H8β	H4β, H5β, H8β
27	1.15, s, 3H	14.8 (CH_3)		H9β, H11	H8β, H12β, H14
28	1.17, s, 3H	18.1 (CH_3)			H13α, H16, H17β
29	1.22, s, 3H	19.4 (CH_3)			
30α	4.09, br. d, 1 H (14.3)	62.9 (CH_2)	H30β	H22, H24αβ	H24β, H30β
30β	4.21, br. d, 1 H (13.5)		H30α		H22, H30α
OCH_3	3.26, s, 3H	56.4 (CH_3)		H22	H22, H24α
15-OH	3.11, br. s, 1 H				
18-OH	3.55, br. s, 1 H		H18		

[a] Spectra were recorded at 25 °C. Chemical shift values are in parts per million (ppm) relative to the residual $CHCl_3$ (δ = 7.25 ppm) or $CDCl_3$ (δ = 77.0 ppm) signals. [b] ^{13}C NMR multiplicities were obtained from APT experiments. [c] Protons correlated to carbon resonances in the ^{13}C column. Parameters were optimized for $^{2,3}J_{C,H}$ = 6 and 8 Hz. [d] Signal recorded as a broad, low-intensity resonance line.

cally, ^{13}C NMR chemical shifts were used to validate the theoretical models, and dipolar coupling correlations derived from 2D-NOESY NMR experiments were used to corroborate the arrangements suggested by QM methods and to determine the relative configuration of the molecule. Because all the proton and carbon values had been confidently assigned by 2D-NMR experiments (Table 1) and were in agreement with the proposed structure **1**, we confined our study to the four possible diastereomers based on C15 and C22 (see stereoisomer models **1a**–**1d** in Figure 3), the two most flexible and thus potentially compromising stereocenters in aplysqualenol A. To determine the relative configuration of these centers the ^{13}C NMR isotropic shifts of each diastereomer (Figure 3) at its lowest-energy configuration were calculated. The minimum-energy configuration for each isomer was identified by a Monte Carlo conformational search with the MMFF force field as implemented in the Spartan 04 software package.[16] All diastereomers were further optimized at the HF/6-31G(2d,p) level of theory with the aid of the Gaussian 03 program.[17] NMR chemical shifts were calculated by the GIAO method at the mPW1PW91/6-31G(2d,p) level of theory. Bifulco and co-workers recently reported that this level of theory gave reasonable results for ^{13}C NMR shifts of organic compounds.[7,18] The experimentally measured values were plotted against the calculated shifts, and a least-squares fit line was determined. The calculated shifts for each isomer were corrected by using the slope and intercept to give scaled ^{13}C

NMR chemical shifts. The difference plots were determined by subtracting the corrected shifts from the experimentally determined ones.

Diastereomer **1b** presented the best ^{13}C NMR chemical shift correlation with the theoretical values (Figure 4) with an average of $\Delta\delta$ = 2.9 ppm (Table 3). It also resulted in the

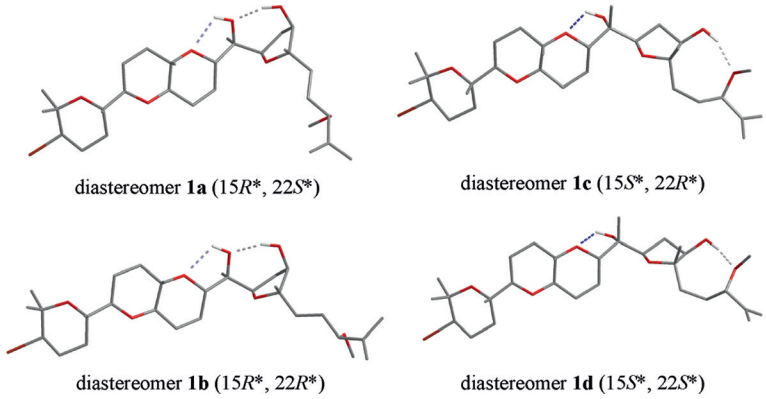

Figure 3. Minimum-energy configurations of the four stereoisomer models **1a**–**1d** considered for quantum mechanical calculations of ^{13}C NMR isotropic shifts. The hydrogen atoms have been omitted for clarity. Oxygen atoms are indicated in red. Hydrogen bonds are represented as dashed lines between the donor hydrogen atom and the acceptor atom. Bonds with less than ideal geometry are displayed with a blue tint. The intensity of the colour increases as the bond becomes less ideal.

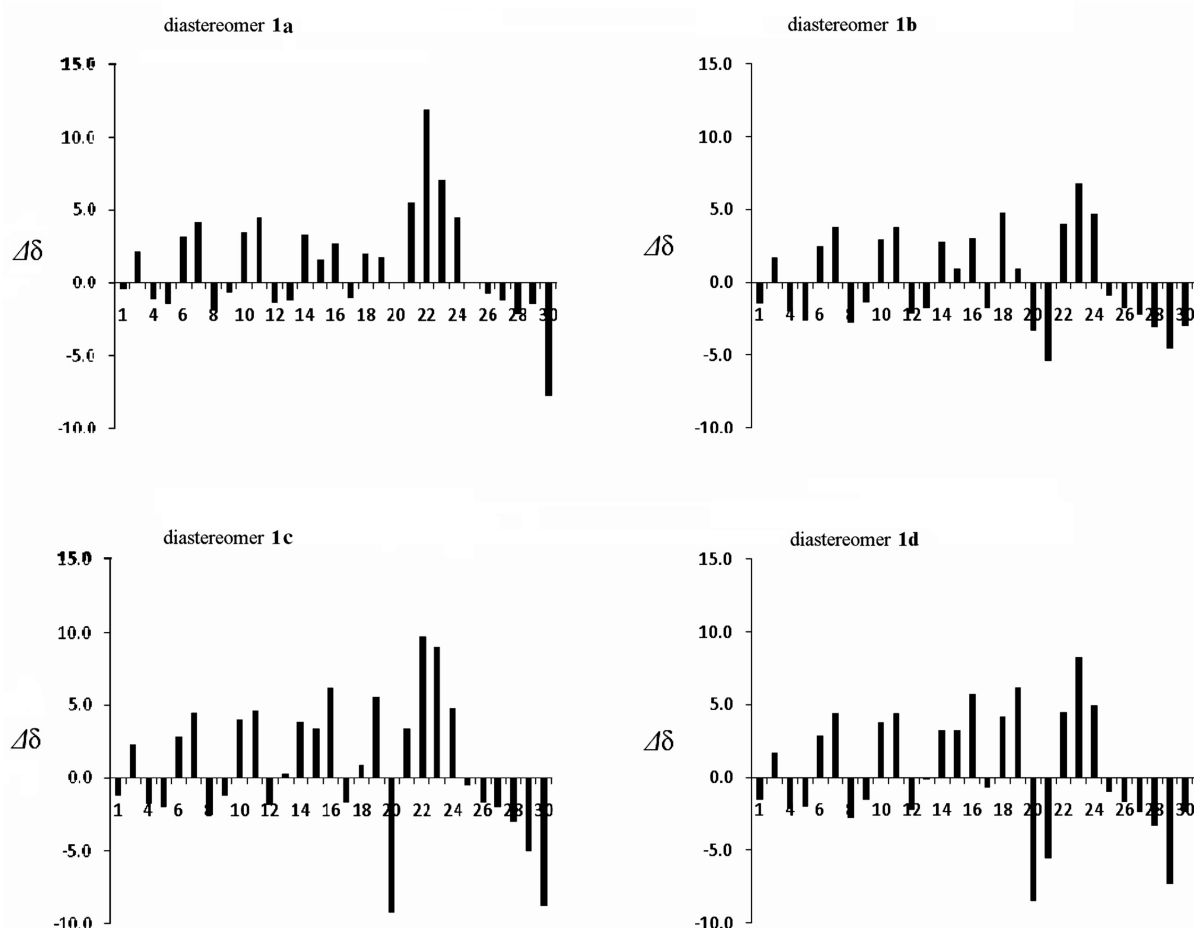

Figure 4. Deviations of the ^{13}C NMR chemical shifts of distereomers **1a**–**1d** from the average. The *x* and *y* axes represent position number and $\Delta\delta$ in ppm, respectively. To discriminate between stereoisomers **1a** and **1b** (the two most likely structures for aplysqualenol A on the basis of the calculation results shown in Table 3), a careful analysis was carried out on individually calculated ^{13}C NMR chemical shifts for C22 and C30, which would be expected to experience larger variations upon inversion of configuration at C22. As shown here, very large differences in the $\Delta\delta$ ^{13}C values of **1a** and **1b** were observed for C22 and C30 (+11.9 vs. +4.0 and –7.8 vs. –3.0, respectively), again suggesting the exclusion of stereoisomer **1a**.

conformation with the lowest energy relative to the other three isomers (**1a**, **1c**, and **1d**). These theoretical results for diastereomer **1b** (15*R**,22*R**) are in agreement with other previously detailed experimental observations, including the observation that the coupling constants of H-22 with the diastereotopic protons H_2-21 are similar, suggesting that the C21–C22 bond experiences free rotation and that the coupling constants are therefore averaged. Had the 18-OH been fixed with the methoxy ether oxygen atom at C22 (diastereomers **1c** and **1d**), two significantly different coupling constant values (one much larger than the other) would have been anticipated. The $\Delta\delta$ values observed for the signals of carbon atoms near the methoxy group at C22 also indicated the (*R**) configuration for this center, as depicted in formula **1**. To summarize, neither diastereomer **1a** (15*R**,22*S**), nor **1c** (15*S**,22*R**), nor **1d** (15*S**,22*S**) is likely to be the correct structure for aplysqualenol A because of the inherently higher relative energies/$\Delta\delta$ values of these compounds. These theoretical calculations not only provided information on the (*R**) configuration of C15 and C22, but also corroborated the arrangement of configuration of C14 depicted in **1** and determined as described above.

Table 3. Calculated parameters for the four diastereomers **1a**–**1d**.

Properties	**1a**	**1b**	**1c**	**1d**
MAE[a]	3.1	2.9	3.9	3.5
Energy[b]	–1741.8144	–1741.8191	–1741.8057	–1741.8125
ΔE[c]	2.98	0	8.42	4.17
R^2[d]	0.9909	0.9982	0.9897	0.9953

[a] Mean absolute error in ppm found for calculated ^{13}C NMR chemical shifts vs. experimental values: MAE = $\Sigma[|(\delta_{exp} - \delta_{calcd})|]/n$. [b] Data in atomic units. [c] Data in kcal mol^{-1}. [d] Correlation coefficient obtained by a linear fit of the calculated (δ_{calcd}) vs. experimental (δ_{exp}) ^{13}C NMR chemical shifts.

From a biogenetic viewpoint the polyoxygenated squalene-derived ethers isolated from *A. dactylomela* could arise from a common precursor: (+)-(10*R*,11*R*)-squalene 10,11-epoxide (**9**, Scheme 1), previously isolated from *Laurencia okamurai*.[19] Upon further oxidation, this compound could give rise to (6*S*,7*S*,10*R*,11*R*,14*S*,15*S*,16*R*,18*R*,19*R*)-16-hydroxysqualene tetraepoxide (**10**; such an intermediate has not been reported yet). The biogenesis of the A–B–C–D ring system could be based on the concerted cyclizations of four epoxides after formation of a bromonium ion at C2–C3, thus forming the framework of these metabolites. In point of fact, the aberrant (*S**) stereochemistry at C14 in compounds **1** and **2** (indicating overall retention of configuration at that center with respect to **10**) indicates that the proposed biogenesis through the cyclization of the squalene tetraepoxide precursor should in fact be concerted. Upon further oxidative metabolism of the remaining olefin, followed by *O*-methylation, aplysqualenol A (**1**) could be obtained (Scheme 1).[20] Compound **1** would in turn be converted into aplysqualenol B (**2**) by enzymatic hydroxylation at C30.

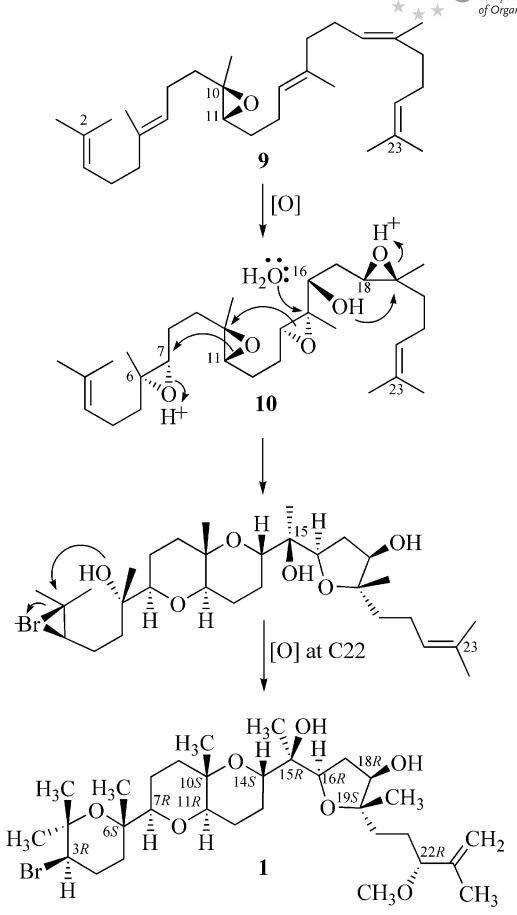

Scheme 1. Proposed biogenetic pathway for aplysqualenol A (**1**).

Conclusions

Aplysqualenols A (**1**) and B (**2**) are novel bromotriterpenes structurally related to thyrsiferol (**5**), which suggests a dietary origin for **1** and **2**. Opisthobranch mollusks belonging to the order *Anaspidea* often feed on red and brown algae, from which they sequester selected bioactive metabolites that are stored in the digestive gland and secreted in the mucus for defensive purposes.[21] The presence of aplysqualenols A and B in *A. dactylomela* thus suggests a likely involvement of these molecules in the chemical defensive mechanism of the sea slug.[7] Squalene-derived polyethers of the type represented by **1** and **2** are currently quite rare, in contrast with thyrsiferol types.[4] The aplysqualenols thus represent the only examples of this small family of marine metabolites to display the (*S**) configuration at C14 and to possess an ether linkage between C16 and C19. The unprecedented (*S**) stereochemistry at C14 leads not only to a conformationally more stable 2,7-dioxabicyclo[4.4.0]decane system (chair/chair B–C ring system) than that present in thyrsiferol (**5**) and its congeners (chair/twist-boat B–C ring system), but also changes the arrangement and direction of the flexible side chain from a less favored axial position to a more stable equatorial orientation.[22,23]

Upon screening in the NCI's in vitro antitumor assay, containing 60 human tumor cell lines, aplysqualenol A (**1**) exhibited inhibitory activity against SNB-19 CNS cancer

and T-47D breast cancer, with IC_{50} values of 0.4 and 0.3 $\mu g\,mL^{-1}$, respectively. To explore its antiviral properties, aplysqualenol A was evaluated against herpes simplex virus type 1 (HSV-1) and type 2 (HSV-2), varicella zoster virus (VZV), human cytomegalovirus (HCMV), and Epstein–Barr virus (EBV). At concentrations above 4 $\mu g\,mL^{-1}$ compound **1** showed a 90% maximal response (EC_{90}) against HSV-1, HSV-2, HCMV, and VZV viruses (acyclovir was used as a control with EC_{50} values of 0.95, 0.95, 0.22, and 0.14 $\mu g\,mL^{-1}$, respectively). Remarkably, aplysqualenol A was very toxic against the Epstein–Barr virus in the VCA Elisa assay ($EC_{90} < 0.08\ \mu g\,mL^{-1}$; acyclovir EC_{50} = 1.1 $\mu g\,mL^{-1}$) with no accompanying toxicity seen in the host Daudi cells.[24] Compounds **1** and **2** showed moderate antiplasmodial activity against *Plasmodium falciparum*, with IC_{50} values of 11 and 18 $\mu g\,mL^{-1}$, respectively. In vitro antituberculosis screening of aplysqualenol A (**1**) against *Mycobacterium tuberculosis* $H_{37}Rv$ at a concentration of 6.25 $\mu g\,mL^{-1}$ showed no inhibitory activity.

Experimental Section

General Experimental Procedures: Optical rotations were measured at the sodium line (589 nm) with a Perkin–Elmer Polarimeter Model 243B. FT-IR spectra were measured with a Nicolet Magna 750 FT-IR spectrophotometer as thin films on NaCl discs. ^1H and ^{13}C NMR spectroscopic data and ^1H-^1H COSY, NOESY, APT, HMQC, and HMBC experiments were measured in $CDCl_3$ with a Bruker Avance DRX 500 FT-NMR spectrometer. ^1H-^1H COSY, NOESY, HMQC, and HMBC spectra were measured with use of standard Bruker pulse sequences. Chemical shifts are given on a δ (ppm) scale with $CHCl_3$ (^1H, δ = 7.26 ppm) and $CDCl_3$ (^{13}C, δ = 77.0 ppm) as the internal standards. Mass spectra were taken at the Mass Spectrometry Laboratory of the University of Illinois at Urbana–Champaign. Column chromatography (CC) was performed on silica gel (35–75 mesh). TLC analyses were carried out with glass silica gel plates, and spots were visualized by exposure to I_2 vapors or by heating of silica gel plates sprayed with H_2SO_4 in EtOH (5%). All solvents were either spectral grade or distilled from glass prior to use. The percentage yield of each compound is based on the weight of the crude MeOH/$CHCl_3$ extract.

Animal Material: Two large specimens of *Aplysia dactylomela* (Rang, 1828, order Anaspidea, superfamily Aplysioidea, family Aplysiidae) were collected on April 28, 2001 in Bahia Salinas, Cabo Rojo, Puerto Rico by hand at 2 feet depth. Each individual was found grazing upon the red alga *Laurencia obtusa*. A voucher specimen has been deposited at the Department of Chemistry, University of Puerto Rico, Río Piedras, Puerto Rico (deposit number ADPR01-1).

Extraction and Isolation of Aplysqualenols A (1) and B (2) and the Known Compound Elatol (11): The organisms were freeze-dried, and the dry animal (54 g dry weight) was cut into small pieces and extracted with $CHCl_3$/MeOH (1:1, 6 × 1 L). The combined organic extracts were concentrated, and the residue obtained (39 g) was suspended in water (500 mL) and partitioned between *n*-hexane, $CHCl_3$, EtOAc, and *n*-butanol. The *n*-hexane extract (11 g) was chromatographed on silica gel (30 g) with *n*-hexane→$CHCl_3$→EtOAc→MeOH in increasing polarity as eluent. The $CHCl_3$ (100%) eluate (980 mg) was chromatographed on silica gel (30 g) with $CHCl_3$ in *n*-hexane (15%) to yield 16 fractions. Subfraction 8 (55 mg) was subsequently chromatographed on silica gel (3 g) with $CHCl_3$ in *n*-hexane (25%) to afford the known elatol (**11**, 37 mg, 0.1% yield).[25] The fraction (1.2 g) that eluted with $CHCl_3$/EtOAc (8:2) was chromatographed on silica gel (31 g) with *n*-hexane in $CHCl_3$ (10%) to afford nine fractions. Subfraction 8 (101 mg) was further purified on silica gel (5 g dry-packed) with elution with EtOAc in $CHCl_3$ (2%). The least polar fraction (66 mg) was purified further by CC on silica gel (5 g) with EtOAc in *n*-hexane (10%) to yield eight fractions. Subfraction 7 (44 mg) was subsequently purified by CC on silica gel (3 g) with EtOAc in *n*-hexane (10%) followed by NP-HPLC [Ultrasphere-Cyano 250 × 10 mm, flow rate: 2.0 mL min^{-1}, UV detection set at λ = 254 nm] with a combination of *n*-hexane/propan-2-ol (95:5) to afford pure aplysqualenol A (**1**, 24 mg). The portion (1.5 g) eluting with EtOAc/MeOH (8:2) was filtered and purified on a Bio-Beads SX-3 column (toluene) to yield three fractions. The second fraction was chromatographed on silica gel (4 g) with MeOH in $CHCl_3$ (0.5%) to afford pure aplysqualenol B (**2**, 7.1 mg).

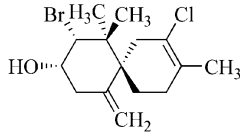

11

Aplysqualenol A (1): Colorless oil. $[\alpha]_D^{20}$ = +48.1 (*c* = 1.6, $CHCl_3$). ^1H NMR ($CDCl_3$, 500 MHz) and ^{13}C NMR ($CDCl_3$, 125 MHz): see Table 1. IR (film): $\tilde{\nu}_{max}$ = 3418, 3072, 2984, 2954, 2875, 1738, 1648, 1456, 1379, 1323, 1127, 1098, 905, 761 cm^{-1}. EIMS: *m*/*z* (%) = 536 [M – HBr]$^+$ (12), 505 (4), 503 (4), 423 (2), 405 (15), 403 (14), 387 (12), 385 (10), 361 (7), 359 (6), 323 (12), 305 (8), 291 (3), 289 (4), 279 (8), 247 (10), 245 (9), 225 (15), 214 (17), 207 (44), 205 (41), 182 (24), 153 (100), 125 (59), 109 (64), 85 (36). HR-FAB-MS (3-NBA): calcd. for $C_{31}H_{53}{}^{79}BrO_7Na$ [M + Na]$^+$ 639.2872; found 639.2858 (Δ = 1.4 mDa).

Aplysqualenol B (2): Colorless oil, $[\alpha]_D^{20}$ = +27.1 (*c* = 1.4, $CHCl_3$). ^1H NMR ($CDCl_3$, 500 MHz) and ^{13}C NMR ($CDCl_3$, 125 MHz): see Table 2. IR (film): $\tilde{\nu}_{max}$ = 3408, 2978, 2952, 2862, 1726, 1453, 1381, 1130, 1095, 1059, 1032, 911 cm^{-1}. HR-FAB-MS (3-NBA): calcd. for $C_{31}H_{54}{}^{79}BrO_8$ [M + H]$^+$ 633.3002; found 633. 3003 (Δ = –0.1 mDa).

Elatol (11): The $[\alpha]_D^{20}$, UV (MeOH), ^1H and ^{13}C NMR, and HR-EI-MS data were identical in all respects to those previously reported.[25]

Acetylation of Aplysqualenol A (1): Compound **1** (1.7 mg, 0.003 mmol) was dissolved in a mixture of dry pyridine (500 μL) and acetic anhydride (500 μL) and heated to 55 °C for 5 h. The cooled reaction mixture was concentrated in vacuo, and the obtained oily residue was purified by CC on silica gel (1 g) with MeOH in $CHCl_3$ (1%) to yield pure aplysqualenol A acetate (**3**, 1.7 mg, quantitative yield). Compound **3**: $[\alpha]_D^{20}$ = +56.0 (*c* = 1.0, $CHCl_3$). ^1H NMR ($CDCl_3$, 500 MHz) and ^{13}C NMR ($CDCl_3$, 125 MHz): see Table 4 in the Supporting Information. IR (film): $\tilde{\nu}_{max}$ = 3549, 3071, 2983, 2951, 2858, 2819, 1740, 1454, 1380, 1242, 1125, 1099, 1029, 921 cm^{-1}. HR-EI-MS: calcd. for $C_{33}H_{54}O_8$ [M – HBr]$^+$ 578.3819; found 578.3826 (Δ = –0.7 mDa), 578 (18), 405 (7), 403 (7), 387 (5), 385 (4), 361 (5), 359 (5), 323 (8), 256 (11), 224 (26), 207 (42), 205 (42), 153 (59), 125 (72), 120 (94), 118 (100), 117 (57).

Acetylation of Aplysqualenol B (2): Aplysqualenol B (3.0 mg; 0.005 mmol) was dissolved in a mixture of dry pyridine (500 μL)

and acetic anhydride (500 μL) and then stirred at 25 °C overnight. The reaction mixture was concentrated in vacuo, and the obtained oil was purified by CC on silica gel (1.0 g) with MeOH in $CHCl_3$ (0.5%) to afford aplysqualenol B diacetate (**4**, 3.0 mg, 88% yield). Compound **4**: colorless oil. $[a]_D^{20}$ = +44.0 (*c* = 0.5, $CHCl_3$). ^1H NMR ($CDCl_3$, 300 MHz) and ^{13}C NMR ($CDCl_3$, 75 MHz): see Table 5 in the Supporting Information. IR (film): $\tilde{\nu}_{max}$ = 3541, 3467, 3087, 2987, 2951, 2869, 2859, 2821, 1740, 1655, 1459, 1440, 1380, 1242, 1121, 1097, 1054, 1029, 922 cm^{-1}. HR-ESI-MS: calcd. for $C_{35}H_{58}{}^{79}BrO_{10}$ $[M + H]^+$ 717.3213; found 717.3216 (Δ = –0.3 mDa).

Computational Methods: Initially, a Monte Carlo (MC) multiple-minimum search with the MMFFs force field was conducted to make a full exploration of the conformational space for all the four possible stereoisomers based on the C15 and C22 stereocenters of aplysqualenol A (**1**). The molecular mechanics MC conformational search employs an algorithm as implemented in the Spartan 04 software package. All the stereoisomers thus obtained were further subjected to ab initio quantum chemical geometry optimizations at the HF/6-31G(2d,p) level of theory. The ab initio calculations were carried out with a Linux AMD64 1.8 GHz instrument with use of the Gaussian 03 program package.[17] The Gaussian 03 uses an expansion of molecular orbitals in atomic-centered Gaussian basis sets such as the double-zeta plus polarization 6-31G(2d,p). NMR shielding tensors were computed with the gauge-independent atomic orbital (GIAO) method at the hybrid density-functional mPW1PW91/6-31G(2d,p) level of theory.

Biological Screening Assays: For a general description of the approach used by the NIAID's Antimicrobial Acquisition and Coordinating Facility (AACF) for determining antiviral activity and toxicity for herpes viruses, visit: http://niaid-aacf.org/protocols/Herpes.htm. Anticancer activity screening by the Developmental Therapeutics Program (DTP) of the National Cancer Institute is conducted by this general protocol: most of the compounds screened have no antiproliferative activity (up to 85%). In order to avoid screening of inactive compounds across all the cell lines, a prescreen is carried out with three highly sensitive cell lines (breast MCF-7, lung NCI-H640, CNS SF-268). Antiproliferative activity must be seen in these cell lines in order to continue to the 60-cell line panel. The 60 different human tumor lines are incubated with five different doses of compound, and a sulforhodamine blue (SRB) assay is performed after 48 h to determine cytotoxicity. From the five-point curve, the following concentrations are extrapolated: GI_{50} (inhibits growth by 50%), TGI (totally inhibits growth), LC_{50} (kills 50% of cells). For the specific screening methods from the DTP website, visit: http://www.dtp.nci.nih.gov/branches/btb/ivclsp.html. Compounds shown to have anticancer activity in cell lines within the NCI 60 panel may then move on to animal trials and if successful, may eventually move on to be tested in clinical trials. Additional experimental details for our primary in vitro antimicrobial assays against *Mycobacterium tuberculosis* and *Plasmodium falciparum* have been described previously.[26,27]

Supporting Information (see footnote on the first page of this article): ^1H and ^{13}C NMR spectra and representative 2D NMR spectroscopic data (^1H-^1H COSY, HMQC, HMBC, and NOESY) for compounds **1** and **2**. Complete ^1H and ^{13}C NMR spectroscopic data for aplysqualenol A acetate (**3**) and aplysqualenol B diacetate (**4**). Atom coordinates for the minimum energy structures of stereoisomer models **1a**–**1d**, as well as statistical information regarding computational results (such as the calculated ^{13}C NMR chemical shifts, the corrected values, and Δδ).

Acknowledgments

We thank Dr. Mark W. Miller (UPR Institute of Neurobiology) and Dr. Ileana I. Rodríguez (UPR-RP) for providing logistic support during the collection of *A. dactylomela*. The assistance of Juan A. Santana during molecular-modeling studies is gratefully acknowledged. The National Cancer Institute (NCI), the National Institute of Allergy and Infectious Diseases (NIAID), the Tuberculosis/Antimicrobial Acquisition & Coordinating Facility (TAACF), and the Institute for Tropical Medicine and Health Sciences (Panama) provided in vitro cytotoxicity, antiviral, antituberculosis, and antimalarial activity data, respectively. High-resolution EI, ESI, and FAB mass spectral determinations were provided by the Mass Spectroscopy Laboratory of the University of Illinois at Urbana–Champaign. B. V. thanks the UPR-RISE Fellowship Program and the Puerto Rico Cancer Center for financial support. This work was partially supported by the NIH-SCORE Program of the University of Puerto Rico (Grant S06GM08102).

[1] J. W. Blunt, B. R. Copp, W.-P. Hu, M. H. G. Munro, P. T. Northcote, M. R. Prinsep, *Nat. Prod. Rep.* **2009**, *26*, 170–244, and previous articles in this series.
[2] a) M. Wessels, G. M. Konig, A. D. Wright, *J. Nat. Prod.* **2000**, *67*, 920–928; b) T. Dias, I. Brito, L. Moujir, N. Paiz, J. Darias, M. Cueto, *J. Nat. Prod.* **2005**, *68*, 1677–1679; c) E. Manzo, M. L. Ciavatta, M. Gavagnin, R. Puliti, E. Mollo, Y. W. Guo, C. A. Mattia, L. Mazzarella, G. Cimino, *Tetrahedron* **2005**, *61*, 7456–7460.
[3] N. R. Ferrigni, B. N. Meyer, J. E. Putnam, L. B. Jacobsen, D. E. Nichols, J. L. McLaughlin, *J. Med. Plant Res.* **1982**, *45*, 31–34.
[4] J. J. Fernández, M. L. Souto, M. Norte, *Nat. Prod. Rep.* **2000**, *17*, 235–246.
[5] J. W. Blunt, M. P. Hartshorn, T. J. McLennan, M. H. G. Munro, W. T. Robinson, S. C. Yorke, *Tetrahedron Lett.* **1978**, *19*, 69–72.
[6] S. Sakemi, T. Higa, C. W. Jefford, G. Bernardinelli, *Tetrahedron Lett.* **1986**, *27*, 4287–4290.
[7] E. Manzo, M. Gavagnin, G. Bifulco, P. Cimino, S. Di Micco, M. L. Ciavatta, Y. W. Guo, G. Cimino, *Tetrahedron* **2007**, *63*, 9970–9978.
[8] P. E. Pfeffer, K. M. Valentine, F. W. Parrish, *J. Am. Chem. Soc.* **1979**, *101*, 1265–1274.
[9] Squalene-derived polyethers with the usual (*R**) configuration at C14 (i.e., compounds **5**–**8**) also display H-14 as a doublet of doublets with two markedly different coupling constant values, consistent with a chair/twist-boat B–C ring system. Notwithstanding, the abnormal relative stereochemistry at C14 in **1** is substantiated by noticeable variations in ^{13}C NMR chemical shifts about the 2,7-dioxabicyclo[4.4.0]decane ring. In **1**, for instance, C27 resonates at δ = 14.8 ppm, whereas all related congeners with the usual C14 (*R**) configuration show this signal at $\delta > 20$ ppm. This modification in stereochemistry also causes the C11 resonance to shift downfield (i.e., from δ = 76.3 ppm in **7** to δ = 80.8 ppm in **1**). A reversal in relative stereochemistry at C14 also causes the nearby C28 methyl group in **1** to resonate at δ = 18.1 ppm rather than at δ = 22.9 or 23.0 ppm as seen in **5** and **7**, respectively, in spite of the fact that all three compounds have the C15 (*R**) configuration.
[10] The minimum-energy configuration for **1** was identified by a Monte Carlo conformational search with the MMFF force field as implemented in the Spartan 04 software package (Wavefunction Inc., Irvine, CA).
[11] a) P. Hohenberg, W. Kohn, *Phys. Rev.* **1964**, *136*, B864–B871; b) W. Kohn, L. J. Sham, *Phys. Rev.* **1965**, *140*, A1133–A1138.
[12] We attempted to confirm the proposed structure of aplysqualenol A (**1**) by X-ray crystallography through chemical transformation into a crystalline derivative. Thus, after heating

of a mixture of **1** and 4-bromophenyl isocyanate in toluene for 3 h, the desired carbamate was obtained in excellent yield, but it failed to crystallize in all of the solvents tried.

[13] S. Porto, J. Durán, J. M. Seco, E. Quiñoá, R. Riguera, *Org. Lett.* **2003**, *5*, 2979–2982.

[14] The procedure is based on the binding of MTPA or MPA to a resin in such a way that, when attacked by the chiral molecule (i.e., compound **1**), the reagent part acts as an electrophile and liberates the corresponding ester derivative into the solution, while the solid matrix behaves as the leaving group. The NMR spectra of the expected derivatives are then obtained without any separation, workup, or manipulation.

[15] The observation that acetylation at C18 and C30 of aplysqualenol B takes place readily at 25 °C points to the fact that the hydrogen bonds between the donor hydrogen atoms and the acceptor atoms in **2** have less than ideal geometry.

[16] *Spartan 04 for Macintosh*, Wavefunction Inc., Irvine, CA.

[17] M. J. Frisch, G. W. Trucks, H. B. Schlegel, G. E. Scuseria, M. A. Robb, J. R. Cheeseman, J. A. Montgomery Jr, T. Vreven, K. N. Kudin, J. C. Burant, J. M. Millam, S. S. Iyengar, J. Tomasi, V. Barone, B. Mennucci, M. Cossi, G. Scalmani, N. Rega, G. A. Petersson, H. Nakatsuji, M. Hada, M. Ehara, K. Toyota, R. Fukuda, J. Hasegawa, M. Ishida, T. Nakajima, Y. Honda, O. Kitao, H. Nakai, M. Klene, X. Li, J. E. Knox, H. P. Hratchian, J. B. Cross, C. Adamo, J. Jaramillo, R. Gomperts, R. E. Stratmann, O. Yazyev, A. J. Austin, R. Cammi, C. Pomelli, J. W. Ochterski, P. Y. Ayala, K. Morokuma, G. A. Voth, P. Salvador, J. J. Dannenberg, V. G. Zakrzewski, S. Dapprich, A. D. Daniels, M. C. Strain, O. Farkas, D. K. Malick, A. D. Rabuck, K. Raghavachari, J. B. Foresman, J. V. Ortíz, Q. Cui, A. G. Baboul, S. Clifford, J. Cioslowski, B. B. Stefanov, G. Liu, A. Liashenko, P. Piskorz, I. Komaromi, R. L. Martin, D. J. Fox, T. Keith, M. A. Al-Laham, C. Y. Peng, A. Nanayakkara, M. Challacombe, P. M. W. Gill, B. Johnson, W. Chen, M. W. Wong, C. González, J. A. Pople, *Gaussian 03*, Revision C.02, Gaussian, Inc., Wallingford CT, **2004**.

[18] a) P. Cimino, L. Gómez-Paloma, D. Duca, R. Riccio, G. Bifulco, *Magn. Reson. Chem.* **2004**, *42*, S26–S33; b) G. Bifulco, P. Dambruoso, L. Gómez-Paloma, R. Riccio, *Chem. Rev.* **2007**, *107*, 3744–3779.

[19] a) H. Kigoshi, M. Ojika, Y. Shizuri, H. Niwa, K. Yamada, *Tetrahedron Lett.* **1982**, *23*, 5413–5414; b) L. De Napoli, E. Fattorusso, S. Magno, L. Mayol, *Phytochemistry* **1982**, *21*, 782–784.

[20] Alternatively, the presence of the 22-OCH_3 group could be explained by methanolysis at the C22–C23 epoxide, implying that the genesis of this functionality in **1** and **2** could be artifactual.

[21] C. N. Rogers, R. De Nys, T. S. Charlton, P. D. Steinberg, *J. Chem. Ecol.* **2000**, *26*, 721–743.

[22] Differences in cytotoxicity detected among compounds of this class have been related to the different conformations adopted by the C14 flexible side chain, see: M. Norte, J. J. Fernández, M. L. Souto, J. A. Gavin, M. D. García-Grávalos, *Tetrahedron* **1997**, *53*, 3173–3178.

[23] Parallel configuration determination studies indicate that **1**, with an equatorial arrangement of the C15-to-C24 side chain, is about 8.84 kcal mol^{-1} more stable than its corresponding C14 epimer.

[24] Primary Epstein–Barr virus infection in childhood is usually mild but in later life usually manifests as infectious mononucleosis.

[25] a) J. J. Sims, G. H. Y. Lin, R. M. Wing, *Tetrahedron Lett.* **1974**, *15*, 3487–3490; b) A. G. González, J. Darias, A. Díaz, J. D. Fourneron, J. D. Martín, C. Pérez, *Tetrahedron Lett.* **1976**, *17*, 3051–3054.

[26] L. A. Collins, S. G. Franzblau, *Antimicrob. Agents Chemother.* **1997**, *41*, 1004–1009.

[27] Y. Corbett, L. Herrera, J. González, L. Cubilla, T. Capson, P. D. Colley, T. A. Kursar, L. I. Romero, E. Ortega-Barria, *J. Trop. Med. Hyg.* **2004**, *70*, 119–124.

Received: July 13, 2009
Published Online: September 16, 2009

